Noise-Sustained Currents in Quasigeostrophic Turbulence over Topography

Alberto Alvarez*, Emilio Hernández-García*#, and Joaquín Tintoré*#
*Departament de Física, Universitat de les Illes Balears, E-07071 Palma de Mallorca, SPAIN
Instituto Mediterráneo de Estudios Avanzados, IMEDEA (CSIC-UIB)
E-07071 Palma de Mallorca, Spain
URL: http://www.imedea.uib.es/
(March 21, 2022)

arXiv:chao-dyn/9701009v1 9 Jan 1997

We study the development of mean structures in a nonlinear model of large scale ocean dynamics with bottom topography and dissipation, and forced with a noise term. We show that the presence of noise in this nonlinear model leads to persistent average currents directed along isobaths. At variance with previous works we use a scale unselective dissipation, so that the phenomenon can not be explained in terms of minimum enstrophy states. The effect requires the presence of both the nonlinear and the random terms, and can be though of as an ordering of the stochastic energy input by the combined effect of nonlinearity and topography. The statistically steady state is well described by a generalized canonical equilibrium with mean energy and enstrophy determined by a balance between random forcing and dissipation. This result allows predicting the strengh of the noise-sustained currents. Finally we discuss the relevance that these noise-induced currents could have on real ocean circulation.

PACS numbers: 05.40.+j, 92.90.+x, 47.27.Eq

I. INTRODUCTION

Under certain conditions, nonlinear interactions are able to organize random inputs of energy into directed motions [1,2]. These ordered fluxes or structures supported by noise have important effects on specific problems in biology [3,4], engineering [5] or physics [6,7]. In fluid dynamics noise appears in a variety of contexts. Thermal fluctuations give rise to Langevin source terms in the equations of motion [8,9], while stirring forces can be modeled as stochastic terms forcing the fluid motion [10]. Noise terms have also been used in modeling short-scale instabilities such as the baroclinic instability in geophysical problems [11–13]. A different way in which noise can enter the description of fluid systems is by considering the interactions taking place at scales below the resolution of a computer model. Addition of noise is a (crude) way of including some influence from unresolved scales [11,14].

The influence of small noise on large scale fluid dynamics, far enough from hydrodynamic instabilities and phase transitions, is expected to be small. However we address in this paper a situation in which it has important consequences: the coupling of fluid to bottom topography in ocean dynamics, which is one of the most important but poorly understood factors controlling ocean circulation. We will show that, when interacting with noise, this coupling leads to the development of steady currents, even in the absence of steady forcing. Although our results are derived for a particular quasigeostrophic fluid model, we expect our general conclusions to apply to other problems in which fluid motion occurs on irregular geometries in the presence of noise.

As a first step the work in this paper will be restricted to barotropic, randomly forced, two-dimensional quasigeostrophic turbulence. Several reasons have been considered for this selection. First of all, this framework provides a physical model complex enough to contain some relevant aspects of ocean circulation, but easy enough for allowing physical understanding without the need of too complex numerical experiments (always difficult to interpret). Second, baroclinic nature of ocean circulation can be usefully represented for large scales by randomly forced barotropic models [11]. In these barotropic models, the random forcing formulation is a simple Markovian process that provides a reasonable representation of the baroclinic nonlinear interactions [12,13].

A brief summary of known results relevant to our study follows for completeness. In the last decades much effort has been devoted towards understanding the effects of bottom topography in barotropic models. Most relevant results on this subject can be summarized in the several key works starting by that developed by Salmon et al. [15] where the statistical properties of topographic turbulence neglecting dissipation and forcing were studied. Among their results the demonstration of the tendency to reach a maximum entropy (Gibbs) state characterized by the existence of stationary mean currents following isobaths should be stressed. The role of dissipation was analyzed in [16] using a different approach. In their study viscous damping was hypothesized, due to its selective damping of high wavenumber modes, to drive the flow towards a state of minimum potential enstrophy for a given energy, hence dissipating enstrophy more rapidly than energy which remains almost constant for a long time. This long-lived minimum potential enstrophy state also consists of flow along topographic contours. More recently, stability properties of minimum enstrophy and maximum entropy states and their relationship have been analyzed by Carnevale and Frederiksen [17]. A quantitative theory of time-dependent, forced and dissipative flow over topography was analyzed by Herring [18] who followed the direct interaction approximation

(DIA) [19] and a modified form of the test-field-model turbulent formalisms [20]. He found that in the case of random stirring and viscous topographic turbulence the stationary components of the energy spectrum behaved close to the above mentioned inviscid results of Salmon et al. [15]. A statistical theory simpler than DIA was used in [21] to investigate the time evolution of the energy and vorticity-topography correlation spectrum. His results also show the emergence of steady circulation for a certain range of the parameters of the theory. As a first step towards understanding the more complicated baroclinic case, Treguier [22] made an extensive exploration of the parameter space for barotropic turbulence. Her numerical results show a non-monotonic dependence of the percentage of steady currents on the forcing, viscous and topography parameters. In some simulations where random forcing and dissipation were considered, these steady currents resemble the simple inviscid solution found in [15].

All these previous studies address the existence of stationary currents following isobaths in a variety of conditions involving random noise. However from these studies it is not possible to infer a clear relation between noise and the physical nature of these currents. The reason is that scale selective (i.e., viscosity) dampings were considered so that the generation of directed currents can be explained in terms of minimum enstrophy states [16]. This physical mechanism involving minimum enstrophy solutions does not require the existence of noise.

In this paper, we try to highlight the role of noise in the appearance of steady currents in such open systems. The main difference with previous studies is that we have considered topographic turbulence damped by Rayleigh friction (bottom friction) instead of viscosity damping. This introduces important physical differences because Rayleigh friction provides a scale-unselective way of dissipating energy from the system and thus does not produce transient minimum enstrophy states. In this way, avoiding one of the possible mechanisms for explaining the mean flows that were present in the simulations of [18], [21] and [22], we show that the combined effect of noise and nonlinear terms is enough to generate mean flows when bottom topography is present. In order to get a more physical understanding of this phenomenon, we show that this current formation at large scales is described, to a good degree of approximation, by a generalized canonical distribution in which the mean enstrophy and the mean energy are fixed by the balance between random forcing and dissipation. Then we suggest that the generation of currents by noise in this system can be understood as arising from the tendency of the large scale fluid motions in our model to approach equilibrium-like states, that is states with the maximum possible entropy consistent with given constraints. However, the non-equilibrium character of our system is reflected in the small scales, which depart from this equilibrium-like state.

Two comments are in order: First, since our motivation is the understanding of large scale ocean circulation, we are interested in the final asymptotic behavior of the fluid system under forcing and dissipation, and not in the approach to it. Therefore the numerous studies available for freely decaying turbulence can not be applied to this problem. Second, the presence of topography introduces spatial scales into the problem so that mechanisms related to scale-invariant wavenumber cascades [23] can not be as relevant here as in a flat bottom situation.

The paper is organized as follows: in Section II the quasigeostrophic model is introduced and numerically solved to show the appearance of directed currents along the topography. Section III contains analytical considerations showing the relevance of the nonlinear terms, discussion of the Fokker-Planck equation for the model and calculation of some average values. The generalized canonical distribution is also presented and some consequences are derived from it. Section IV checks the validity of the canonical description. Discussion of the results and their implications for large-scale ocean modelling are in Section V.

II. THE MODEL AND THE NOISE-SUSTAINED CURRENTS

The quasi-geostrophic evolution equation for the streamfunction $\psi(x,y,t)$ describing flow over topography is given by [24]:

$$\frac{\partial \nabla^2 \psi}{\partial t} + \mathcal{J}\left(\psi, \nabla^2\psi + h'\right) = -\epsilon \nabla^2 \psi + F \ , \qquad (1)$$

where

$$\mathcal{J}\left(A,B\right) \equiv \hat{\mathbf{k}} \cdot \left(\nabla A \times \nabla B\right) \qquad (2)$$

ϵ^{-1} is the bottom friction decay time, $h' = f\Delta H/H_0$ with f the Coriolis parameter (that will take the value $10^{-4}s^{-1}$ as appropriate for mean latitudes), H_0 the mean depth, and $\Delta H(x,y)$ the local deviation from this mean depth. $\hat{\mathbf{k}}$ is the unit vector normal to the horizontal plane (x,y), $\times$ denotes the cross vector product and $F(x,y,t)$ is a Gaussian white-noise process with zero mean and correlations $\langle F(x,y,t)F(x',y',t')\rangle = D\delta(x-x')\delta(y-y')\delta(t-t')$. It represents relative-vorticity random forcing. Eq.(1) is to be solved in a square domain with boundary conditions such that ψ vanishes at the boundaries. The streamfunction ψ gives the horizontal components of the fluid velocity $(u(x,y), v(x,y))$ as

$$u = -\frac{\partial \psi}{\partial y} \ , \quad v = \frac{\partial \psi}{\partial x} \qquad (3)$$

In order to solve (1) we have used the quasi-geostrophic numerical scheme developed in [25] on a grid of 128×128 points. The resolution of our scheme (corresponding to the distance between grid points) is of 10 km, so that the total system size is $L = 1280$ km. The algorithm,

based on finite differences and the leap-frog algorithm, keeps the value of energy and enstrophy constant when it is run in the inviscid and unforced case. The consistent way of introducing the stochastic term into the leap-frog scheme can be found following the lines of [26,27]: Basically, a field of Gaussian random numbers is generated at each time step, and the random field added to the deterministically evolved vorticity field at each time step is the sum of the field generated at this time step plus the field generated at the previous time step. The random number generator employed in the simulation is detailed in [28]. The amplitude of the forcing, $D = 2 \times 10^{-9}\ m^2/s^2$, and the e-folding decay constant, $\epsilon = 3 \times 10^{-7} s^{-1}$ of the damping mechanism have been chosen in order to obtain final velocities of several centimeters per second. The topographic field (Fig 1) is randomly generated from a isotropic spectrum containing, with equal amplitude and random phases, all the Fourier modes corresponding to scales between 80 km and 300 km. The model was run for 5×10^5 time steps (corresponding to 126 years) after a statistically stationary state was reached. The average streamfunction was then computed from the configurations obtained every time step.

The results obtained from this numerical experiment show the generation of a stationary mean flow correlated with bottom topography and with velocity values of order of 3 cm/s (Fig. 2). This numerical result indicates the existence of a physical mechanism, different from the minimum enstrophy tendency addressed in [16], that is able to organize random inputs of energy in a mean state different from rest characterized by currents with a clear dependence with bottom topography. The mean currents will advect any neutral tracer with them, so that the kind of motion so generated is very similar to the phenomena described in [1–6]. In addition we have checked by Fourier analysis that the temporal series of $\psi(x, y, t)$ at fixed space point (x, y) is roughly periodic in time (but quite noisy), so that there are also directed currents in the phase space of ψ. In the next section we try to clarify the possible origin of the currents.

III. ANALYTIC APPROACHES

A. The linear model

As a first step to investigate the emergence of these noise induced currents, we will explore the solutions of the linearized dynamics. Neglecting the nonlinear term, Eq. (1) transforms into:

$$\frac{\partial \nabla^2 \psi}{\partial t} + \hat{\mathbf{k}} \cdot (\nabla \psi \times \nabla h') = -\epsilon \nabla^2 \psi + F \ , \tag{4}$$

After ensemble averaging Eq. (4) over noise realizations we obtain the equation that determines the stationary state of the linear system:

$$\hat{\mathbf{k}} \cdot (\nabla \langle \psi \rangle \times \nabla h') + \epsilon \nabla^2 \langle \psi \rangle = 0 \tag{5}$$

No stationary solution of Eq. (5) can be a function of topography. This is because a functional dependence of the mean streamfunction on the bottom topography implies that the first term of (5) would be identically zero and then $< \psi >$ should be a solution of Laplace's equation. With the boundary conditions used, this implies that the mean streamfunction vanishes in every point of the system. Thus in the linear model (4) the forcing generates small excursions of $< \psi >$ around the rest state, in a way unrelated to topography. In conclusion, the nature of noise sustained currents is thus determined not only by the random noise but also by the nonlinear interactions.

B. The Fokker-Planck equation of the nonlinear model

As it was shown from the study of the linearized dynamics, the nonlinear term is needed in order to get mean stationary solutions different from rest. This fact implies to consider the full dynamics given by (1). Due to the stochastic nature of the system we will explore the statistics of its solutions in phase space. To do that, the Fokker-Planck equation (FPE) of the probability distribution of the field solution of Eq. (1) will be derived. From the standpoint of treating the statistics of an ensemble of solutions of (1), it is convenient to represent the streamfunction $\psi(x, y, t)$ as a linear combination of orthogonal eigenfunctions of the Laplacian satisfying the adequate boundary conditions:

$$\psi(x, y, t) = \sum_i A_i(t) \phi_i(x, y), \quad \nabla^2 \phi_i(x, y) = -\alpha_i^2 \phi_i(x, y) \tag{6}$$

$$\int_S dx dy \phi_i(x, y) \phi_j(x, y) = S \delta_{ij} \tag{7}$$

The integral is over the whole two-dimensional domain, of area $S = L^2$.

The evolution equation for the amplitude factors $A_i(t)$ reads:

$$\alpha_k^2 \dot{A}_k - \sum_{ij} \beta_{ijk} \left(\alpha_j^2 A_j A_i - A_i h'_j \right) = -\epsilon \alpha_k^2 A_k + \alpha_k f_k \tag{8}$$

where:

$$\alpha_k f_k = -\frac{1}{S} \int_S dx dy \ F(x, y, t) \phi_k(x, y) \ , \tag{9}$$

$$\langle f_k(t) f_{k'}(t') \rangle = \frac{D}{S \alpha_k \alpha_{k'}} \delta_{kk'} \delta(t - t') \ , \tag{10}$$

and

$$\beta_{ijk} = -\frac{1}{S}\int_S dxdy\ \hat{\mathbf{k}}\cdot\left(\nabla\phi_i(x,y)\times\nabla\phi_j(x,y)\right)\phi_k(x,y)\ . \tag{11}$$

Some properties of the nonlinear interaction coefficients β_{ijk} are that they vanish if any two indexes are equal, they are invariant under cyclic permutation of indices, and they reverse sign under non-cyclic permutation of indices [29].

In order to use the symmetries and asymmetries of Eq. (8) more clearly, we introduce the following change of variables:

$$X_k(t) \equiv \alpha_k A_k(t)\ ,\ h'_j \equiv \alpha_j h_j\ . \tag{12}$$

The equation is now:

$$\dot{X}_k(t) = N_k - \epsilon X_k(t) + f_k(t) \tag{13}$$

where:

$$N_k = \sum_{ij}\frac{\beta_{ijk}\alpha_j^2}{\alpha_j\alpha_i\alpha_k}\left(X_iX_j - X_ih_j\right) \tag{14}$$

Now, we consider the amplitudes $\{X_i\}$ of the orthogonal modes as the coordinates of a point (in an infinite-dimensional phase space) whose position corresponds to the state of a particular realization at a single instant in time. Since $f_k(t)$ is white noise (Eq. (10)), the continuity equation for the phase space probability density $\rho = \rho(\{X_i\},t)$ takes the Fokker-Planck form [30]:

$$\frac{\partial\rho}{\partial t} + \sum_k\frac{\partial}{\partial X_k}\rho\left(N_k - \epsilon X_k\right) = \sum_k\mu_k\frac{\partial^2\rho}{\partial X_k^2} \tag{15}$$

where $\mu_k = D/(2S\alpha_k^2)$ and represents a diffusion coefficient for the $k-$mode. We can see from (15) that random forcing acts as a diffusion mechanism for the probability density in phase space. This mixing character is opposite to the term represented by friction that tends to drive the system towards the origin of the phase space, the rest state.

The FPE (15) can be easily integrated in the stationary state if the potential condition:

$$\frac{\partial Z_k}{\partial X_l} = \frac{\partial Z_l}{\partial X_k} \tag{16}$$

with $Z_k = \mu_k^{-1}\left(N_k - \epsilon X_k\right)$ holds [30]. Otherwise there is no simple way of finding the stationary probability distribution. The potential condition is not satisfied in the case described by (15) so that some assumptions must be performed to get an approximate probability distribution for the stationary state.

However the FPE can be still useful for determining some average quantities needed below. The average of any phase space function $F(\{X_k\})$ satisfy the adjoint of Eq.(15), or *backwards* equation [30]. This can be shown by multiplying (15) by $F(\{X_k\})$, integrating over phase space, and using integration by parts. For stationary averages ($\frac{\partial\rho}{\partial t} = 0$), the result is

$$\int d\Gamma\left(\frac{\partial F}{\partial X_l}\left(N_k - \epsilon X_k\right) + \mu_k\frac{\partial^2 F}{\partial X_k^2}\right)\rho = 0 \tag{17}$$

$\int d\Gamma$ denotes integration over phase space $\int\prod_k dX_k$. Choosing $F = \frac{1}{2}\alpha_k^2\left(\frac{1}{2}X_k - h_k\right)^2$, substituting into (17) and summing over k, the antisymmetric terms containing β_{ijk} disappear and we find:

$$\epsilon\sum_k\alpha_k^2\left\langle\left(\frac{1}{2}X_k - h_k\right)X_k\right\rangle = \sum_k\frac{1}{2}\mu_k\alpha_k^2 \tag{18}$$

where $< ... >$ indicates average over the stationary distribution ρ. The term between brackets is related to the mean potential enstrophy, so that Eq. (18) gives an expression for this quantity in terms of the damping coefficient ϵ and the noise intensity μ_k. Similarly, by choosing $F = \frac{1}{4}X_k^2$ and repeating the procedure above we find:

$$\epsilon\sum_k\alpha_k^2\left\langle\frac{1}{2}X_k^2\right\rangle = \sum_k\frac{1}{2}\mu_k \tag{19}$$

This relates the mean energy $\left\langle\frac{1}{2}X_k^2\right\rangle$ to ϵ and μ_k.

C. A generalized canonical equilibrium

Properties of the stationary state of the FPE (15) can be used to obtain an approximate expression for the probability distribution. As it was shown in [15], invariance of energy and potential enstrophy has important implications on the inviscid and unforced dynamics. In particular statistical properties can be correctly computed by assuming that at long times the system explores completely, or at least samples with enough significance, the hypersurface of constant energy and potential enstrophy (for a discussion see [32]). When damping is introduced, the system will be brought to the vicinity of the rest state in phase space. But random forcing will keep some motion present. Since the effect of the nonlinear terms in the unforced and undamped dynamics was to drive the system along the intersection of the constant-energy and constant-potential-enstrophy hypersurfaces, it is then reasonable to expect that in the presence of forcing and damping evolution will proceed on average close to the hypersurfaces of mean constant energy and mean potential enstrophy determined by the damping and forcing coefficients through equations (18) and (19). If this hypothesis holds, the most likely probability distribution compatible with such constraints, that is the one obtained from the maximization of the entropy functional $S[\rho] = \int\prod_k dX_k\rho(\{X_k\})\log\rho(\{X_k\})$ subjected to the constraints (18) and (19), should be an approximation to the real stationary probability distribution [31].

The validity of the heuristic considerations above, as the validity of general statistical mechanics arguments in any interesting physical situation, would be hard to establish rigorously. In our case, justification of our assumptions will come from comparisons with numerical simulations. Ergodicity, or at least efficient sampling of the constant energy and potential enstrophy hypersurfaces would be certainly more justified here than in the unforced case because of the additional mixing tendency provided by random forcing.

Entropy maximization subjected to constraints (18) and (19) leads formally to the same expression as in the inviscid and unforced case, that is, the predicted probability distribution is:

$$\rho(\{X_k\}) = \prod_k \rho_k(X_k), \tag{20}$$

with

$$\rho_k(X_k) \ = e^{\left(-\frac{1}{2}\left(a+b\alpha_k^2\right)X_k^2+\alpha_k^2 h_k b X_k\right)} \tag{21}$$

a and b are the Lagrange multipliers enforcing the constraints. Although this expression is formally identical to the inviscid one, there is an important difference: In the inviscid case the Lagrange multipliers are determined from the initial values of energy and enstrophy, whereas here the dependence on the initial state is asymptotically lost and (21) refers to the final state in which the Lagrange multipliers are determined by the mean values of energy and enstrophy. Their exact values are given in (18) and (19) in terms of the forcing and friction parameters present in the original equation (1). The values of the first and second moments of X_k obtained from (21) are given by:

$$\langle X_k \rangle = \frac{\alpha_k^2 h_k b}{a + b\alpha_k^2} \tag{22}$$

$$\left\langle X_k^2 \right\rangle = \frac{1}{a + b\alpha_k^2} + \frac{\alpha_k^4 h_k^2 b^2}{a + b\alpha_k^2} \tag{23}$$

These equations in conjunction with (18) and (19) allow the determination of the Lagrange multipliers a and b from the parameters in the FPE or in (1). Alternatively, they relate the Lagrange multipliers with quantities measurable from simulation or experiments.

As in the inviscid case, equations (22) and (23) imply the existence of a mean circulation controlled by the topography [15]. To see that we focus on the value of the first moment which is specially interesting since it describes the generation of mean flows following isobaths. This becomes evident rewriting (22) in terms of the Fourier amplitudes of the functional expansion (6):

$$\langle A_k \rangle = \frac{h_k' b}{a + b\alpha_k^2} \tag{24}$$

that in the physical space imply the relation:

$$\nabla^2 \langle \psi \rangle + h' = c \langle \psi \rangle \tag{25}$$

where $c = a/b$. This linear relationship between the mean potential vorticity and the mean streamfunction implies, considering that for large scale motions the relative vorticity is smaller than the ambient one ($\nabla^2 \langle \psi \rangle \ll h'$), that $\langle \psi \rangle$ is proportional to h', that is $\langle \psi \rangle$ describes mean flows following the isobaths. We have checked that the distribution (20)-(21) is not an exact solution of the FPE (15). In the following Section however we show that it gives a good description of the large scale average properties.

IV. COMPARISON WITH NUMERICAL SIMULATIONS

The correlation between topography and mean streamfunction, as predicted by (25) is obvious by comparing Figs. 1 and 2. The agreement can be made more quantitative by plotting $\nabla^2 \langle \psi \rangle + h'$ versus $\langle \psi \rangle$, both obtained from the numerical simulation. This is done in Fig 3. Eq. (25) predicts a linear relationship. Fig. 3 shows a clear linear trend but there is also an evident scatter in the data that will be commented below. The linear correlation coefficient is 0.940. Further analysis of the validity of theoretical predictions can be done by fitting the data in Fig. 3 to Eq. (25) to get a numerical value for the constant c. This procedure gives a value of $c = (5.30 \pm 0.02) \times 10^{-9}\, m^{-2}$. The predicted value of c obtained from (22) and (23) by considering the magnitudes of the mean energy and potential enstrophy obtained in the stationary state is $5.5 \times 10^{-9} m^{-2}$ which represents a deviation of 4% with respect to the value obtained by numerical simulation. In order to test if such deviations occur at all scales, we have computed the power spectrum of the fields $(\nabla^2 \langle \psi \rangle + h')/c$ and $\langle \psi \rangle$, both obtained from the numerical model, and compared them with the energy spectrum of the field $\langle \psi \rangle$ computed from direct resolution of (25) which will be taken as reference spectrum. Theory predicts that these distributions should be the same. Fig. 4 shows that there is very good agreement between numerical results and the theoretical spectrum obtained from the canonical probability distribution at low wavenumbers (large scales) where topography components are relevant. The most important deviations occur at small scales. There are also much smaller discrepancies at very low wavenumbers, that is at basin scales, similar to the ones observed when analyzing the equilibrium solutions of purely inviscid two-dimensional turbulence [33]. The reason for them could be the long dynamical time scale of large-scale eddies that implies very long equilibration times [33]. The deviations involving small scales cannot be explained by relaxation-time arguments. These scales are clearly out of equilibrium. This absence of equilibrium at least at small scales could be expected from arguments based on turbulent cascades: In two-dimensional turbulence an enstrophy flux towards small scales is expected [34]. Since Rayleigh friction is not as

effective in dissipating vorticity at small scales as viscosity would be, an accumulation of enstrophy is expected at the largest wavenumbers, and this is in fact seen in Fig. 4. In contrast, equations (20)-(21) predict that states with vorticity at wavenumbers above a cut-off are forbidden. This is easy to see from the canonical partition function of the system, that can be written as:

$$Z(b,a) = \int \mathcal{D}\psi \; e^{-\frac{a}{2}(\int dxdy(\nabla\psi)^2 + l^2 \int dxdy\left(\nabla^2\psi + h'\right)^2)} \tag{26}$$

where $l^2 = b/a = c^{-1}$ has units of length square and $\int \mathcal{D}\psi$ denotes functional integration. If $\nabla^2\psi + h'$ varies on length scales smaller than l the second term of the exponential dominates and all the microstates of the system with these characteristics are dropped out from the ensemble averages. As a result properties of scales near or smaller than the cut-off cannot be well described by the canonical probability distribution.

The fact that small scales are responsible for the broadening of the linear tendency in Fig. 3 can be verified from the fact that the linear correlation coefficient between mean potential vorticity and mean streamfunction fields after scales smaller than 100 km (i.e. several times the cut-off scale) have been filtered out is 0.975, higher than the original one. Finally, if all scales except those with relevant topographic components ($100 - 400$ km) are removed, correlation coefficient increases until a value of 0.982, that is, the agreement with theory predictions is even better. In conclusion the canonical distribution given by (20)-(21) is a good description of the numerical results for length scales larger than 100 km.

V. DISCUSSION

In this paper, we have focussed our attention on the effects that noise produces on a simplified stochastic quasigeostrophic model where only friction and random terms have been considered. The reason for our interest comes from indications of generation of currents along isobaths in randomly forced quasigeostrophic systems presented in previous works [18,21,22]. Since the main interest of those works was not the study of the effect of random forcing on flow with underlying topography, the formulations used there included several effects absent in our model. In particular numerical experiments were carried out in the presence of correlated noise and scale-selective dampings. This more complex framework makes it difficult to identify unambiguously the basic physical mechanisms producing the currents. In particular the introduction of viscosity or bi-laplacian damping generates decaying minimum enstrophy states described by [16] that obscure the effects of noise highlighted in our work. Our use of bottom friction as a damping mechanism tries to isolate the effect that noise could produce on the dynamics by avoiding minimum enstrophy states.

As a result of our study, we have found that the random term supplies energy to the system and contributes (together with the nonlinear term) to the mixing of the probability density in phase space. This compensates the reducing volume tendency of the dissipation term. When this compensation occurs the system dynamics resembles the behaviour developed by the isolated system, that is without forcing and damping. The physical effect of this phase space dynamics is the generation of a stationary state characterized by mean fluid motions following isobaths. We can conclude then that these mean currents are noise-sustained and come from the interaction of random noise with the nonlinear term. The existence of bottom topography is relevant in order to get a mean component in the spectrum, that is, to develop mean currents in the basin. This result seems to indicate that noise could play a relevant role in maintaining the mean component of planetary motions when bottom topography is present. A remaining open question is however, how much of the currents observed in [18,21,22] is produced by random terms and how much is related to the minimum enstrophy tendency that is certainly present in their models. Our isolation of the effects of noise is a first step to evaluate the relative importance of both effects.

One of the state of the art questions on the study of large scale ocean circulation and modeling is related to the effects that unresolved scales might have on the larger scale dynamics. The range of scales which numerical models can handle explicitly is limited by the actual computer power, the large size of the global domain and the time characteristics of climatic studies (long-time simulations). These limitations prevent us from simulating the small and large scale features simultaneously. However, it is also well known that some of these unresolved processes produce significant influences on the large scale circulation. The influence of small scales must then be introduced through some parametrization.

A natural way of considering the unresolved dynamics would be to include the small and fast oceanic processes as some kind of random noise in the deterministic models of large scale phenomena. In general, dealing with ocean modeling the action of small scales is only considered as an enhancement of the viscosity coefficient (the so called eddy-viscosity). Random noise is usually neglected from oceanic calculations because it is assumed that its presence produces a negligible effect on large scale ocean dynamics.

Although the full ocean dynamics is characterized by the existence of three-dimensional motions, for sufficiently large spatial scales (scales larger than several hundreds of kilometers) and long time behaviour (more than one week) the ocean can be well described by quasigeostrophic dynamics including bottom topography. The results shown here could be a first basis from which to conjecture that the origin of some observed large scale ocean structures are due to phenomena which are several orders of magnitude smaller than the structures themselves. The experimental determination of this conjec-

ture can be very difficult to carry out due to the broad range of spatial and temporal scales in ocean. However, new approaches for future studies where large scale stochastic primitive equation models are used, instead of purely deterministic ones, could be a reasonable way to go deeper into the problem. Effectively, inclusion of noise in a coarse-resolution primitive equation model as a representation of the small scale processes that are not well resolved would provide a mechanism for the model to generate noise-sustained large scale currents along isobaths in a natural way, that obviously would be missing in a deterministic version of such a model. Ad-hoc inclusion of currents along isobaths has been already shown to improve results of coarse-resolution numerical models [36,37]. Presently, general ocean circulation models are deterministic. However, based on the results established on this paper it seems reasonable to hypothesize that stochastic models will provide more realistic answers about ocean dynamics and more concretely about the possible existence and relevance of these noise-sustained currents in the real ocean.

ACKNOWLEDGMENTS

Financial support from CICYT (AMB95-0901-C02-01-CP and MAR95-1861), DGICYT (PB94-1167 and PB94-1172), and from the MAST program MATTER MAS3-CT96-0051 (EC) is greatly acknowledged.

[1] J. Maddox, Nature **369**, 181 (1994).
[2] C. R. Doering, W. Horsthemke, J. Riodan, J. Phys. Rev. Lett. **72**, 2984 (1994).
[3] J. Maddox, Nature **368**, 287 (1994).
[4] J.K. Douglass, Lon Wilkens, Eleni Pantazelou, Frank Moss, Nature **365**, 337 (1993).
[5] S. M. Bezrukov, Igor Vodyanoy, Nature **378**, 362 (1995).
[6] J. Rousselet, L. Salome, A. Ajdari, J. Prost, Nature **370**, 446 (1994).
[7] R.J. Deissler, J. Stat Phys. **40**, 376 (1985); ibid. **54** 1459 (1989).
[8] L.D. Landau and E.M. Lifshitz, *Fluid mechanics. Second Edition. Course of theoretical physics, vol. 6*, Pergamon Press (New York, 1987).
[9] M. Treiber, Phys. Rev. **E 53**, 577 (1996), and references therein.
[10] W.D. McComb, Rep. Prog. Phys. **58**, 1117 (1995).
[11] G. P. Williams, J. Atmos. Sci. **35**, 1399 (1978).
[12] S. F. Edwards, J. Fluid Mech. **18**, 239 (1964).
[13] C. E. Leith, J. Atmos. Sci. **28**, 145 (1971).
[14] P.J. Mason, Q.J.R. Meteorol. Soc. **120**, 1 (1994).
[15] R. Salmon, G. Holloway, M.C. Hendershot, J. Fluid Mech. **75**, 691 (1976).
[16] F.P. Bretherton, D.B. Haidvogel, J. Fluid Mech. **78**, 129 (1976).
[17] G.F. Carnevale, J. S. Frederiksen, J. Fluid Mech.**82**, 747 (1987).
[18] J.R. Herring, J. Atmos. Sci.**34**, 1731 (1977).
[19] R. H. Kraichnan, J. Fluid Mech. **5**, 497 (1971).
[20] R. H. Kraichnan, J. Fluid Mech. **47**, 513 (1971).
[21] G. Holloway, J. Phys. Oceanogr. **8**, 414 (1978).
[22] A.M. Treguier, Geophys. Astrophys. Fluid Dynamics **47**, 43 (1989).
[23] G.F. Carnevale, J.C. McWilliams, Y. Pomeau, J.B. Weiss, W.R. Young, Phys. Fluids **A 4**, 1314 (1992).
[24] J. Pedlosky, *Geophysical fluid dynamics*, Springer-Verlag (New York, 1987).
[25] P. F. Cummins, J. Mar. Res. **50**, 545 (1992).
[26] J.M. Sancho, M. San Miguel, S. Katz, J. Gunton, Phys. Rev. **A 26**, 1589 (1982).
[27] A. Greiner, W. Strittmatter, J. Honerkamp, J. Stat. Phys. **51**, 95 (1988).
[28] R. Toral, A. Chakrabarti, Computer Phys. Comm. **74**, 327 (1988).
[29] P.D. Thompson, J. Fluid Mech. **55**, 711 (1972).
[30] C.W. Gardiner, *Handbook of stochastic methods for Physics, Chemistry and the Natural Sciences*. Springer-Verlag (New York ,1989).
[31] A. Katz, *Principles of statistical mechanics*, W.H. Freeman & Co. (San Francisco, 1967); W.T. Grandy *Foundations of statistical mechanics*, Kluwer (Dordrecht, 1987).
[32] J.Miller, P.B. Weichman, M.C. Cross, Phys. Rev. **A 45**, 2328 (1992).
[33] D.G. Fox, S.A. Orszag, Phys. Fluids **16**, 169 (1973).
[34] R.H. Kraichnan, Phys. Fluids **10**, 1417 (1967).
[35] G. Holloway, J. Phys. Oceanogr. **22**, 1033 (1992).
[36] A. Álvarez, J. Tintoré, G. Holloway, M. Eby, J.M. Beckers, J. Geophys. Res., **99**, 16053 (1994).
[37] M. Eby, G. Holloway, J. Phys. Oceanogr. **24**, 2577 (1994).

FIG. 1. Depth contours of a randomly generated bottom topography. Maximum depth is 381.8m and minimum depth -381.8m over an average depth of 5000m. Levels are plotted every 63.6 m. Continuous contours are for positive deviations with respect to the mean, whereas dashed contours are for negative ones.

FIG. 2. Mean streamfunction computed by time averaging when a stationary state has been achieved. Maximum and minimum values are 1120.2 and -1120.2 m^2/s. Levels are plotted every 186.7 m^2/s. Continuous contours denote positive values of the streamfunction, whereas dashed contours denote negative ones. The resemblance to Figure 1 is evident.

FIG. 3. Scatter plot of mean potential vorticity versus mean streamfunction obtained from numerical simulation. A gross linear tendency appears that resembles the linear tendency observed in inviscid calculations. Each symbol is obtained from a different position in the simulation domain.

FIG. 4. Comparison, as a function of the radial wavenumber index $L\alpha_k/2\pi$, of the power spectra of $(\nabla^2 \langle\psi\rangle + h')/c$ (dash-dot line), $\langle\psi\rangle$ (dashed line), both obtained from numerical simulation, and the power spectra of the solution $\langle\psi\rangle$ of Eq. (25) (solid line).

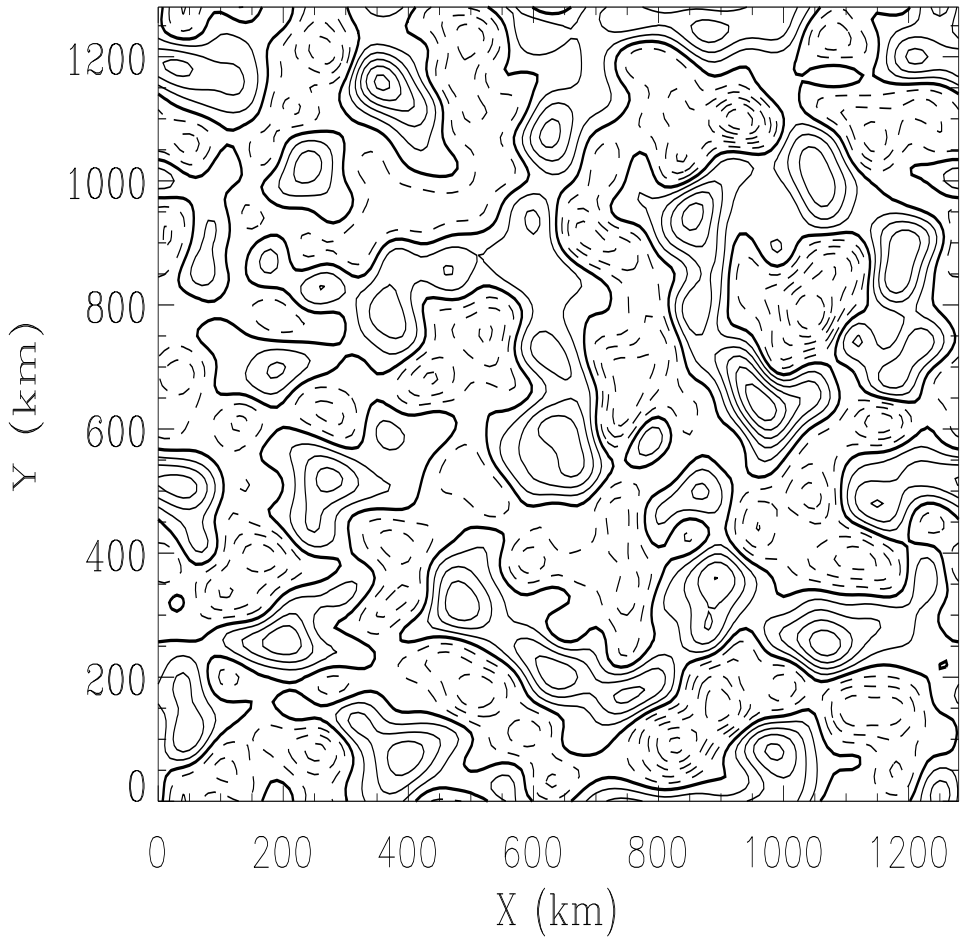


Figure 1, Noise –sustained currents..., by Alvarez et al

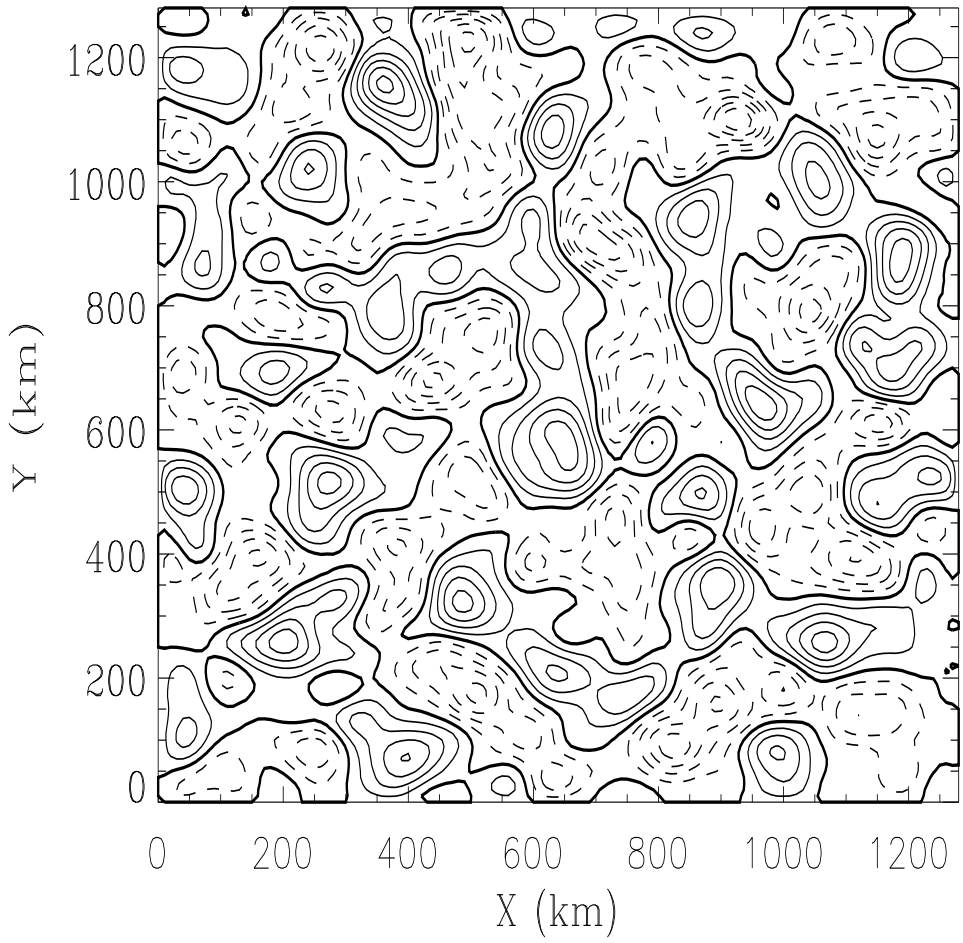


Figure 2, Noise–sustained currents..., by Alvarez et al

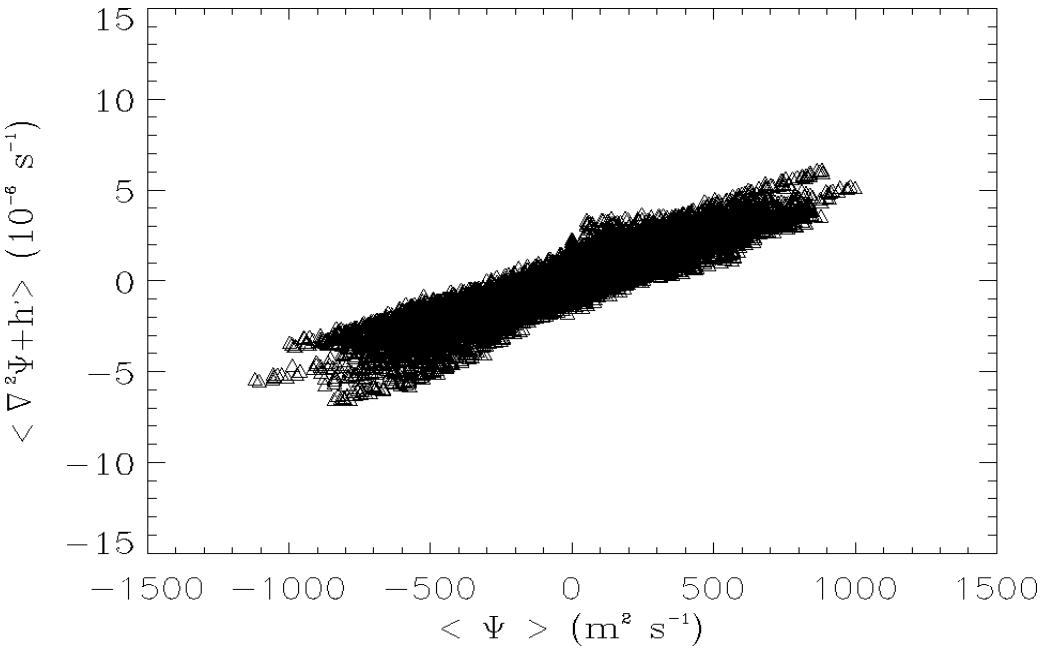


Figure 3, Noise−sustained currents..., by Alvarez et al

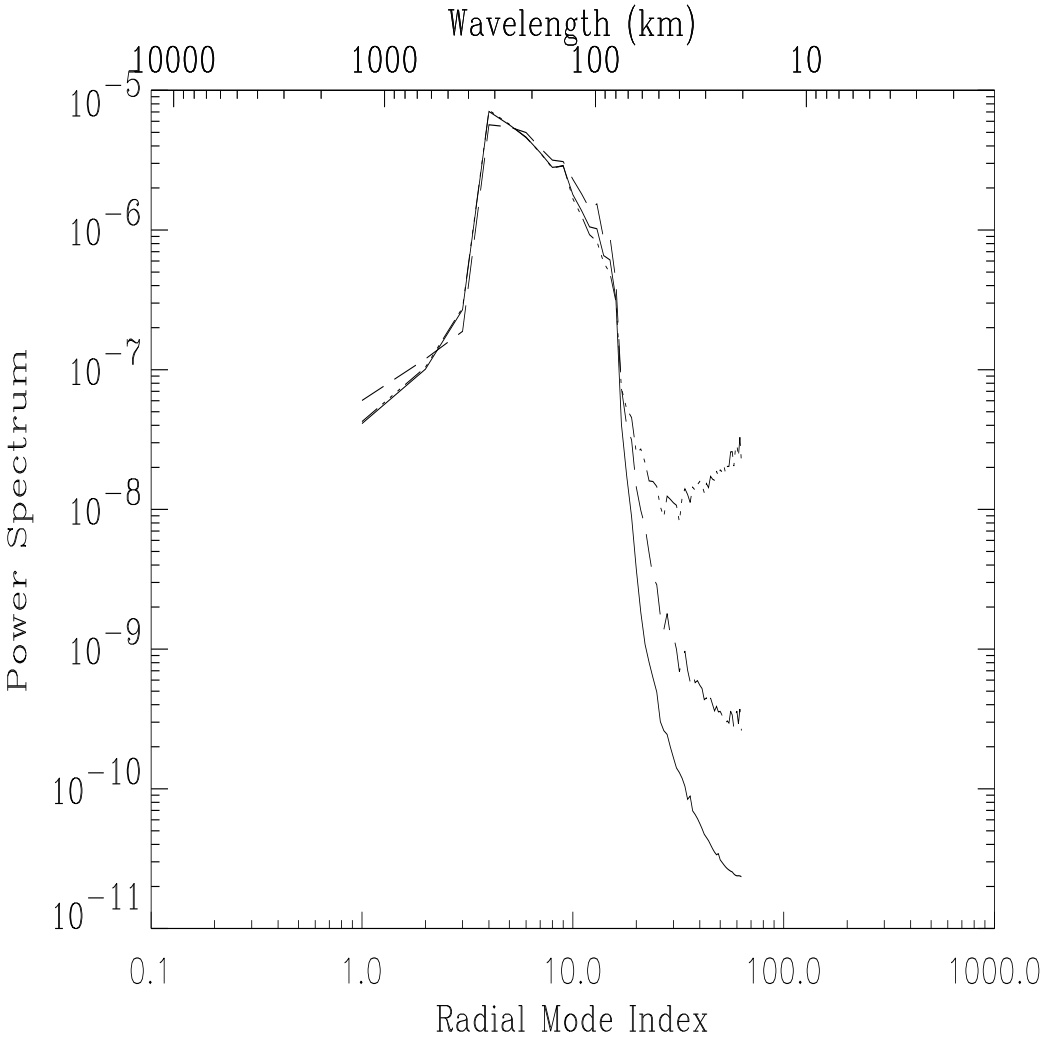


Figure 4, Noise–sustained currents..., by Alvarez et al